HHS Public Access

Author manuscript

Nat Struct Mol Biol. Author manuscript; available in PMC 2015 November 01.

Published in final edited form as:

Nat Struct Mol Biol. 2015 May ; 22(5): 411–416. doi:10.1038/nsmb.3012.

Subunit asymmetry and roles of conformational switching in the hexameric AAA+ ring of ClpX

Benjamin M. Stinson[1], **Vladimir Baytshtok**[1], **Karl R. Schmitz**[1], **Tania A. Baker**[1,2], and **Robert T. Sauer**[1,*]

[1]Department of Biology, Massachusetts Institute of Technology, Cambridge, MA 02139

[2]Howard Hughes Medical Institute, Massachusetts Institute of Technology, Cambridge, MA 02139

Abstract

The hexameric AAA+ ring of *Escherichia. coli* ClpX, an ATP-dependent protein unfolding and translocation machine, functions with the ClpP peptidase to degrade target substrates. For efficient function, ClpX subunits must switch between nucleotide-loadable (L) and nucleotide-unloadable (U) conformations, but the roles of switching are uncertain. Moreover, it is controversial whether working AAA+ ring enzymes assume symmetric or asymmetric conformations. Here, we show that a covalent ClpX ring with one subunit locked in the U conformation catalyzes robust ATP-hydrolysis, with each unlocked subunit able to bind and hydrolyze ATP, albeit with highly asymmetric position-specific affinities. Preventing U⇔L interconversion in one subunit alters the cooperativity of ATP hydrolysis and reduces the efficiency of substrate binding, unfolding, and degradation, showing that conformational switching enhances multiple aspects of wild-type ClpX function. These results support an asymmetric and probabilistic model of AAA+ ring activity.

INTRODUCTION

The hexameric AAA+ ring of *Escherichia coli* ClpX recognizes protein substrates via a peptide degron, uses cycles of ATP binding and hydrolysis to unfold the substrate, and then translocates the denatured polypeptide through an axial pore and into the ClpP degradation chamber, which lies within a barrel-shaped structure formed by the stacking of two heptameric rings[1]. Although ClpX is a homohexamer, biochemical and structural experiments reveal differences among the subunits. For example, some subunits bind nucleotide with higher affinities than others, and some subunits fail to bind nucleotide[2,3]. Crystal structures of ClpX hexamers show two major classes of subunits, typically arranged with approximate two-fold symmetry[3,4]. Four loadable (L) subunits bind nucleotide in the cleft between the large and small AAA+ domains, whereas repositioning of these domains in two symmetrically opposed unloadable (U) subunits destroys the nucleotide-binding site

*corresponding author: bobsauer@mit.edu.

AUTHOR CONTRIBUTIONS

B.M.S., V.B. and K.R.S. designed experiments. B.M.S. performed experiments. B.M.S., T.A.B. and R.T.S. analyzed data and wrote the manuscript. All authors approved the final version of the manuscript.

(Fig. 1a). However, the functional relevance of the pseudo symmetric L4:2U subunit arrangement observed in most crystal structures is unclear. Indeed, biochemical experiments suggest that an L5:1U configuration may predominate in the presence of nucleotide[3]. The issue of subunit symmetry in working hexameric rings applies to other AAA+ enzymes that remodel proteins, as some models require symmetric subunit function[5], and crystal structures of many of these enzymes show 2-fold, 3-fold, or 6-fold symmetry[6].

Previous studies provide evidence that dynamic interconversion between the nucleotide-loadable and nucleotide-unloadable conformations of ClpX subunits is necessary for efficient coupling of ATP hydrolysis to mechanical work[3]. The precise roles of conformational switching, however, remain poorly understood. To address this question, we use crosslinking to prevent U→L switching in one subunit of variants of a covalent ClpX hexamer, and characterize the resulting conformationally restricted enzymes. A ClpX ring with one U-locked subunit catalyzes robust ATP hydrolysis. Experiments examining the nucleotide binding and hydrolytic properties of the unlocked subunits reveal that each one can bind and hydrolyze ATP, albeit with position-specific affinities that are highly asymmetric. U-locking one subunit in the ClpX ring compromises multiple facets of function, including the binding, unfolding, and degradation of protein substrates, and the cooperativity of ATP hydrolysis, U-locking two subunits exacerbates functional defects. These results support an asymmetric and probabilistic model of ring activity and the importance of conformational switching for robust activity. They also constrain models for conformational coordination among ClpX subunits, and illustrate strategies that should be useful for dissection of mechanism in other AAA+ ring systems.

RESULTS

Constraining a subunit to the U conformation by crosslinking

To permit introduction of mutations into specific subunits, we expressed variants from genes encoding three *E. coli* ClpX$^{\Delta N}$ subunits linked into trimers, which form pseudo hexamers[7]. We deleted the family-specific N domain[8] in these experiments, as it interferes with covalent linkage of subunits but is dispensable for interactions with ClpP and degradation of ssrA-tagged substrates[1,7]. To assemble fully covalent hexamers, we linked trimers via sortase ligation[9]. In all subunits, we mutated the only endogenous reactive cysteine (C169S) to allow introduction of specific cysteine substitutions, which we could then modify by bismaleimide crosslinking or attachment to maleimide-conjugated fluorescent dyes.

In ClpX crystal structures, the beta-carbons of residues D144 and K330 are separated by ~13 Å in nucleotide-unloadable (U) subunits and ~27 Å in nucleotide-loadable (L) subunits (Fig. 1b). We introduced the D144C and K330C substitutions into the N-terminal subunit of a covalent ClpX trimer, and crosslinked the cysteines by addition of 1,6-bismaleimidohexane (BMH), which has a length of ~16 Å (Fig. 1c). This distance allows crosslinking of cysteines 144 and 330 in U subunits but is too short for crosslinking in L subunits. Thus, a BMH-crosslinked subunit is locked in the unloadable conformation. We refer to such subunits as “U-locked”. Using the strategy diagrammed in Fig. 1d, we linked this BMH-crosslinked trimer to a parental trimer via sortase ligation to create a covalent hexamer. To determine the degree of crosslinking, we introduced a TEV-protease cleavage site into the

flexible peptide tether between the cysteine-modified subunit and the neighboring subunit (Fig. 1d), allowing resolution of crosslinked and uncrosslinked subunits by SDS-PAGE after TEV cleavage. This assay showed a complete shift in electrophoretic mobility of the modified subunit upon addition of BMH, indicating very efficient crosslinking (Fig. 1e). Modification with *N*-propylmaleimide (NPM, Fig. 1c), which mimics modification by BMH without covalent crosslinking of the two cysteines, did not produce a shift in mobility (Fig. 1e).

To determine if BMH crosslinking of the D144C/K330C subunit disrupted its folding or the integrity of the ClpX ring, we compared the behavior of the parental enzyme and the BMH-crosslinked enzyme by analytical size-exclusion chromatography (Fig. 2a), circular-dichroism spectroscopy (Fig. 2b), and thermal-denaturation experiments in the presence and absence of ATP (Fig. 2c). In each of these assays, the properties of the parental and BMH variants were very similar, strongly indicating that crosslinking does not disrupt the fundamental structure of the ClpX ring.

One U-locked subunit permits robust ATP hydrolysis

We assayed hydrolysis of different concentrations of ATP by covalent hexamers composed of parental C169S ClpX subunits or variants containing a single D144C/K330C subunit modified with BMH or NPM and fit curves to the Hill form of the Michaelis-Menten equation to determine V_{max}, K_M, and the Hill constant (Fig. 3a; Table 1). V_{max} for the BMH variant was ~500% that of the parent. For the NPM variant, V_{max} was intermediate between the parent and BMH suggesting that NPM modification biases subunit conformation without generating a fully U-locked subunit. Parental ClpX displayed strong positive cooperativity in ATP hydrolysis, the NPM variant showed almost no cooperativity, and the BMH variant displayed negative cooperativity (Table 1). Thus, U-locking even one subunit in the ClpX ring alters subunit-subunit communication. K_M for ATP hydrolysis by the parent and NPM variant was ≤ 100 μM but increased to ~4 mM for the BMH variant, presumably as a consequence of faster ATP hydrolysis and/or weaker binding. An unfolded titin^{I27}-ssrA protein substrate substantially stimulated the ATPase activity of the parental enzyme as expected[3,10-12] but did not appreciably stimulate ATP hydrolysis by the NPM or BMH enzymes (Fig. 3b).

ADP inhibition of conformationally restricted variants

ADP is a competitive inhibitor of ATP binding and hydrolysis. To test the possibility that conformational switching helps the ClpX hexamer escape an unproductive ADP-bound state, we measured hydrolysis of 2 mM ATP in the presence of various ADP concentrations (Fig. 3c). For the parental enzyme, ADP stimulated hydrolysis at low concentrations, suggesting that a ring with one or a few bound ADPs is more active, and inhibited hydrolysis at higher concentrations with an IC_{50} of 1.4 mM. By contrast, ADP did not significantly stimulate the NPM or BMH variants and inhibited these variants more strongly with IC_{50} values of 0.5-0.6 mM. Thus, restriction of subunit switching renders the hexamer more susceptible to ADP inhibition.

Subunit-specific nucleotide binding and hydrolysis

How does U-locking of one subunit in the BMH hexamer affect nucleotide binding in the remaining five subunits? To address this question, we measured binding to each unlocked subunit by nucleotide-coordinated metal energy transfer (nCoMET), which measures quenching of a nearby fluorophore upon binding of a nucleotide●Co^{2+} complex[3]. The nucleotide-binding sites in adjacent subunits of ClpX are ~35 Å apart, whereas the Co^{2+} metal only quenches fluorophores within ~25 Å[3,13]. Thus, judicious placement of a fluorophore in one subunit permits measurement of nucleotide binding to just that subunit. For these studies, we constructed and purified five variants of BMH hexamers in which a single unlocked subunit contained an M363C substitution (see Online Methods for construction strategy), which we modified with an Oregon-Green fluorophore. We refer to each unlocked subunit by its numbered position clockwise from the U-locked subunit, as shown in Fig. 4a.

We measured ATP, ATPγS, and ADP binding to the Oregon-Green modified subunits at positions 1-5 of the U-locked variants by nCoMET. Fig. 4a shows apparent ATP, ATPγS, and ADP affinities for each of these subunits, which varied in an asymmetric fashion. Individual ATP-binding curves for each subunit are shown in Fig. 4b. For each nucleotide, the apparent affinity for one Oregon-Green modified subunit of the parental unlocked enzyme (an average over all ring configurations) was similar to the average of the five unlocked subunits in the different BMH variants (Table 2). Importantly, nucleotide bound each unlocked subunit, indicating that they all assume a loadable conformation in some fraction of the population. For ATP and ATPγS, apparent affinities are not equilibrium dissociation constants, as these nucleotides can leave by hydrolysis and product dissociation in addition to simple dissociation. In most cases, ATP and ATPγS bound with similar apparent affinities to a given subunit. However, subunit 2 bound ATP substantially more weakly than ATPγS. Because ClpX hydrolyzes ATP faster than ATPγS[14], which would result in a lower apparent affinity, this difference could arise because subunit 2 hydrolyzes ATP much faster than other subunits or because hydrolysis elsewhere in the ring weakens binding to subunit 2. ADP bound each subunit in the U-locked hexamer with tighter apparent affinities than ATP or ATPγS, which might be expected to lead to more potent ADP inhibition than that observed in the Fig. 3c experiment. It is possible, however, that ATP binds more tightly or ADP binds more weakly to a ClpX hexamer with some ATP-bound and some ADP-bound subunits.

We measured Co^{2+}-supported ATP hydrolysis by the parental and BMH enzymes (Fig. 4c) for comparison with the nCoMET results. Previous studies suggest that occupancy of weak ATP-binding sites is necessary for robust ATP hydrolysis by ClpX[3]. Consistently, the K_M for ATP hydrolysis for the parental enzyme (~170 μM) was higher than the average affinity measured by nCoMET (~100 μM). This difference was more extreme for the U-locked BMH variant, with a K_M in excess of 1 mM compared to an average affinity of ~110 μM. Although the nCoMET assay measures binding to specific subunits, it does not reveal the degree of saturation of any single subunit. Notably, both the ATPase and nCoMET binding curves for the U-locked variants were negatively cooperative. Even though each unlocked subunit binds nucleotide in some fraction of the population, it is plausible that negative

cooperativity prevents any single hexamer from binding four or five nucleotides and hydrolyzing ATP efficiently except at very high concentrations.

To assess the importance of ATP hydrolysis in different subunits of BMH ClpX, we introduced single E185Q (EQ) Walker-B mutations to inactivate ATP hydrolysis[2] in subunits 1, 2, 3, 4, or 5 in different U-locked BMH variants. Each single EQ mutation decreased the maximal ATP-hydrolysis rate relative to the BMH hexamer, suggesting that each unlocked subunit contributes to hydrolysis (Fig. 4d). The dependence of hydrolysis on ATP concentration was negatively cooperative for variants with EQ mutations in subunits 1, 2, or 5 and non-cooperative for subunits 3 and 4 (Table 1), suggesting that these mutations affect subunit-subunit communication in a position-specific manner.

U-locking impairs substrate binding and degradation

We assayed binding of a native titin^{I27}-ssrA protein substrate labeled with a BHQ3 quencher to fluorescent variants of BMH ClpX, NPM ClpX, or the parental enzyme. Compared to the parent, the BMH and NPM variants showed substantially weaker binding and lower levels of maximal quenching (Fig. 4a), suggesting that NPM modification and U-locking hinder binding of protein substrates.

U-locking did not substantially affect binding to the ClpP peptidase. As assayed by changes in the tryptophan fluorescence emission spectrum, the BMH and NPM enzymes bound Y60W ClpP in a manner similar to parental ClpX (Fig. 5b). In combination with ClpP, the NPM variant degraded unfolded titin^{I27}-ssrA protein at ~50% of the parental rate and the BMH variant degraded this substrate at ~15% of the parental rate (Fig. 5c). Thus, U-locking one subunit of the ClpX ring diminishes but does not prevent substrate engagement and translocation into ClpP. Notably, however, degradation by ClpP and the BMH enzyme was much less energetically efficient than degradation by the NPM or parental enzymes in terms of the number of ATP molecules hydrolyzed per substrate degraded (Fig. 5d), suggesting that many power strokes in the U-locked enzyme do not result in productive work. In assays of degradation of a native substrate (Arc-Gcn4-ssrA), the NPM enzyme had ~40% of the parental activity, whereas the BMH hexamer had ~10% activity (Fig. 5e). Relative to the parental enzyme, the BMH enzyme degraded the native substrate less efficiently than the unfolded substrate, suggesting that U-locking impairs protein unfolding.

Double U-locked variants

We also constructed a variant in which two symmetrically opposed subunits in the ClpX ring harbored the D144C and K330C substitutions to allow crosslinking with BMH or modification with NPM. Compared to variants containing only one modified subunit, the variants containing two modified NPM or BMH subunits had lower V_{max} values for ATP hydrolysis and were even more impaired in degradation (Fig. 6). These results suggest that increasing the number of U-locked subunits exacerbates functional defects.

DISCUSSION

In the presence of an unfolded protein substrate, U-locked BMH ClpX hydrolyzes ATP at a rate similar to the parental enzyme but degrades the substrate at a ~6-fold slower rate. Thus,

the majority of ATP-hydrolysis events in the modified enzyme appear to be uncoupled from power strokes that result in mechanical work. A similar uncoupling of most power strokes from machine function is observed when disulfide bonds lock one or two ClpX subunit in the L conformation[3]. These results emphasize the importance of U⇔L conformational switching in the ClpX ring for robust mechanical activity.

U-locking of a single subunit alters communication between subunits and interferes with normal coordination of ATP hydrolysis. For example, ATP hydrolysis by the parental enzyme shows modest positive cooperativity, whereas hydrolysis by the U-locked BMH variant is negatively cooperative. Positive cooperativity might normally result from conversion of a subunit with low ATP affinity to one with high affinity as a consequence conformational switching. ATP hydrolysis by the BMH variant is also inhibited at lower ADP concentrations than the parental enzyme, suggesting that U-locking may slow ADP ejection from ClpX subunits that need to be cleared and reloaded with ATP before mechanical work can continue.

Restricting a single subunit in the ClpX ring to the U conformation affects binding to protein substrates, reducing both the apparent affinity and the extent of binding at substrate saturation. As substrate engagement appears to be a slow step in ClpXP degradation[15], these changes in substrate binding almost certainly contribute to the defects in degradation of unfolded substrates by BMH ClpX and ClpP. However, the defects in native substrate unfolding and degradation are larger than expected from the reduced fraction of substrate bound at saturation. Thus, restricting the conformation of one ClpX subunit to a U conformation seems to reduce the rate at which native substrates can be unfolded and then degraded. Population and single-molecule studies indicate that multiple ClpX power strokes are required, on average, before unfolding of a native substrate occurs[12,15-18]. Moreover, stably folded substrates are often released from ClpX when an unfolding attempt fails[19]. Thus, it is plausible that the unfolding defect caused by U-locking is related to the substrate-binding defect. Specifically, more frequent release of native substrates from U-locked ClpX after a failed power stroke would result in weaker observed binding and require a larger number of rebinding events, on average, prior to successful unfolding. Restrictions in subunit conformation caused by U-locking might prevent the enzyme from readjusting its grip on an engaged substrate, leading both to the defects in substrate binding and unfolding, either because U⇔L switching is abolished and/or because other important conformational states become inaccessible.

In the ClpX variants used here, the N domain was deleted to allow linkage into covalent hexamers. Although the N domain is essential for binding of some substrates[1,20], $ClpX^{\Delta N}$ supports ClpP degradation of ssrA-tagged substrates as well as full-length ClpX[7]. Thus, the basic operating principles for mechanical work revealed by our studies are likely applicable to the wild-type enzyme. Nonetheless, our results do not preclude a role for the N domain in U⇔L conformational switching.

Most crystal structures of ClpX hexamers have four L subunits and two U subunits, arranged with approximate 2-fold symmetry as shown in Fig. 1a[3,4]. Whether this 4L:2U arrangement represents a “working” configuration has been questioned, as experiments based on contact

quenching of rhodamine dyes support the presence of a 5L:1U hexamer in the presence of nucleotide, protein substrate, and ClpP[3]. Although our results do not settle this issue, restricting one subunit in the ClpX ring to the U conformation, as expected in a 5L:1U ring, allows robust ATP hydrolysis and permits the unfolding and degradation of protein substrates, albeit at diminished levels compared to wild type presumably because U⇔L switching is compromised. By contrast, restricting two opposed subunits to the U conformation, as expected in a pseudo symmetric 4L:2U ring, abolishes most ATP hydrolysis and accompanying mechanical activity.

How subunits with different ATP-binding and hydrolysis properties are arranged and coordinated in working AAA+ hexamers is controversial. For example, studies with the AAA+ PAN and 26S Rpt_{1-6} unfolding rings have been interpreted as support for a model in which high-affinity, moderate-affinity, and ATP-free subunits are always arranged with two-fold symmetry around the hexameric ring but interconvert or switch in a strictly sequential fashion[5]. If ClpX functioned according to this model, then the subunit opposite the U-locked subunit in BMH ClpX should be forced into an ATP-free U conformation. However, our nCoMET results show that this subunit binds ATP, ADP and ATPγS, with affinities similar to or tighter than neighboring subunits. Our experiments also show that this subunit contributes to ATP hydrolysis. Finally, the pattern of nucleotide affinities that we measure for different subunits in the BMH hexamer is inconsistent with functional symmetry of any type in the hexameric ring of ClpX. Similarly, asymmetry in the Rpt_{1-6} unfolding ring of the 26S proteasome is supported both directly by EM structures and indirectly by biochemical experiments analyzing the functional contributions of specific subunits[21-23].

Because ClpX rings with only one or two hydrolytically active subunits are active in substrate unfolding and degradation, Martin et al. proposed an asymmetric and probabilistic model of ring function[8]. Single-molecule optical trapping studies of ClpXP unfolding and translocation provide strong support for this model[12,15-18] as do our current studies. For example, we find that each unlocked subunit in a ClpX ring with one U-locked subunit can bind and hydrolyze ATP with some probability. Thus, ATP hydrolysis is not restricted to a subset of subunits at certain positions in the ring relative to the U-locked subunit. Our current and prior results[3] also show that subunits in the ClpX ring must be able to switch between U and L conformations to allow efficient substrate binding, unfolding, and degradation. Switching may ensure that the machine is both robust to failure by ejecting improperly bound nucleotides and opportunistic by allowing well-positioned subunits to switch into conformations allowing productive contacts with protein substrate.

ONLINE METHODS

Materials

PD buffer contained 25 mM HEPES (pH 7.0), 100 mM KCl, 10 mM $MgCl_2$, and 10% (v/v) glycerol). IEXA, IEXB, and IEXC buffers contained 20 mM HEPES (pH 7.8), 0.5 mM EDTA, 10% (v/v) glycerol, 1 M urea, with 150 mM KCl, 500 mM KCl, or 20 mM KCl, respectively. Xlink buffer contained 20 mM HEPES (pH 7.8), 300 mM KCl, 0.5 mM EDTA, and 10% (v/v) glycerol. ATP (Sigma), ADP (Sigma), and ATPγS (Roche) were dissolved in PD buffer and adjusted to pH 7.0 by addition of NaOH. Alexa 555 C_2

maleimide (Molecular Probes), Alexa 647 C_2 maleimide (Molecular Probes), Oregon Green 488 maleimide (Molecular Probes), and BHQ3 carboxylic acid succinimidyl ester (Biosearch Technologies) were dissolved in DMSO and stored desiccated at −20 °C.

Proteins

All ClpX variants were derived from *E. coli* $ClpX^{\Delta N}$ (residues 61-424), contained a C169S substitution to remove an accessible cysteine, and were constructed by polymerase chain reactions. Linked ClpX trimers were purified using Ni-NTA and Superdex-200 chromatography generally as described[8]. Superdex-200 chromatography was carried out in Xlink buffer, and fractions containing ClpX were concentrated with Millipore Amicon 10,000 MWCO spin concentrators. During purification of variants with reactive cysteines, buffers were supplemented with 0.5 mM ethylenediaminetetraacetic acid (EDTA) and 1 mM dithiothreitol (DTT), kept at 4 °C, degassed, and sparged with argon to minimize oxidation. ClpX concentrations were calculated in pseudo-hexamer equivalents based on absorbance at 280 nm.

NPM- or BMH-modified variants were constructed as shown in Fig. 1d. A pseudo-hexamer consisting of linked ClpX trimer containing the D144C and K330C substitutions in the N-terminal subunit (trimer A) was purified as described above in buffer containing DTT and was desalted into degassed, argon-sparged Xlink buffer using an 10 × 100 mm Sephadex G-25 column, diluted to a concentration of 1 μM pseudo hexamer with Xlink buffer, placed in a 37 °C water bath for ~10 min, and reacted with either 10 μM BMH or 500 μM NPM for 15 min before quenching with 5 mM DTT. The modified samples were then desalted and concentrated. BMH-crosslinking efficiency was assessed by TEV digestion and subsequent SDS-PAGE on a 15% polyacrylamide gel. Digestion reactions contained 1 μM modified pseudo hexamer and equimolar TEV and were digested with equimolar TEV at room temperature for 30 min before quenching with SDS-sample buffer (final concentrations 50 mM Tris-HCl pH 6.8, 2% SDS, 10% glycerol, 1% β-mercaptoethanol, 0.02% bromophenol blue). Double NPM and double BMH pseudo hexamers were dimers of the modified trimers described above.

An evolved *S. aureus* sortase-A enzyme with P94S/D160N/K194T substitutions[24] was used to ligate trimer A, which contained a C-terminal LPETG sortase recognition site, to one of several different linked trimers that contained an N-terminal poly-glycine motif after TEV protease cleavage (trimer B). These experiments rely on dissociation of pseudo-hexamers into trimers and reassembly. Trimer-B variants were desalted after initial Ni-NTA chromatography, cleaved with equimolar TEV at room temperature for 2 h, passed over a small Ni-NTA column to remove H_6-tagged TEV, and further purified by Sephadex-200 chromatography. One subunit of trimer B contained a M363C substitution for nCoMET experiments, a D170C substitution for substrate-binding experiments, or an E185Q mutation for ATP-hydrolysis experiments. For fluorophore-labeled ClpX variants, prior to sortase ligation, linked trimers stored in DTT were desalted and reacted with a 3-fold excess of the appropriate maleimide-functionalized fluorophore at room temperature for 30 min before quenching with 1 mM DTT and desalting into Xlink buffer using a PD10 column (GE Healthcare). For nCoMET experiments, trimer A constructs contained a BMH modification

in either the first or third subunit, and trimer B constructs contained the M363C-Oregon Green modification in the first, second, or third subunit. For example, the ClpX variant with subunit 1 labeled (Fig. 3a) was constructed from trimer A with the BMH modification in the third subunit and trimer B with the fluorophore in the first subunit, and the subunit-5 variant contained BMH in the first subunit of trimer A and the fluorophore in the third subunit of trimer B. ClpX variants with single E185Q mutations were constructed similarly. For substrate binding experiments, the first subunit of trimer A contained the BMH modification and the first subunit of trimer B contained the Alexa 555 modification.

Sortase-ligation reactions contained 5 μM trimer A, 5 μM trimer B, and 1 μM sortase, and were carried out at room temperature for 2-4 hours in Xlink buffer supplemented with 5 mM $CaCl_2$ and 1 mM DTT. Reactions were then diluted 5-fold with IEXC buffer and chromatographed on a Source 15Q column (GE Healthcare) using a linear gradient from 100% IEXA buffer to 100% IEXB buffer. The presence of 1 M urea in the chromatography buffers was required to separate fully covalent hexamers from linked trimers. Fractions containing fully linked hexamers were identified by SDS-PAGE, concentrated, and desalted into Xlink buffer. The parental ClpX variant was constructed as described above with otherwise unmodified trimers A and B and had ATPase and degradation activities similar to other $ClpX^{\Delta N}$ pseudo hexamers.

ClpP and $titin^{I27}$-ssrA variants were purified as described[12,25]. Unfolded $titin^{I27}$-ssrA was prepared by reacting native cysteines with either fluorescein-iodoacetamide or iodoacetic acid as described[12]. For $titin^{I27}$-ssrA binding experiments, PCR mutagenesis was used to mutate the GLG linker between the $titin^{I27}$ sequence and the ssrA tag to GCG. Purification buffers for this variant were designed to minimize oxidation as described above for reactive-cysteine ClpX preparations. 1.0 equivalents of BHQ3 carboxylic acid succinimidyl ester was reacted with 0.9 equivalents of 2-maleimidoethylamine (Sigma) and 1.0 equivalents of triethylamine for 2 h at room temperature in DMSO. Cys-containing $titin^{I27}$-ssrA was desalted and reacted with a 3-fold excess of the resulting maleimide-functionalized BHQ3 quencher for 30 min at room temperature in Xlink buffer supplemented with 2 mM Tris to quench unreacted BHQ3 carboxylic acid succinimidyl ester and desalted using a PD10 column.

Assays

Unless noted, experiments were performed at room temperature in PD buffer. Fluorescence experiments were performed using a SpectraMax M5 plate reader (Molecular Devices) or a PTI QM-20000-4SE spectrofluorimeter. ATP hydrolysis by ClpX variants was measured by a coupled assay[26]. ADP inhibition of ATP hydrolysis was measured by a colorimetric assay using malachite green in PD buffer lacking glycerol[27]. Reactions were quenched at various time points by addition of EDTA to 20 mM. Solution A was freshly prepared 7.5% (w/v) ammonium molybdate, solution B was 0.122% (w/v) malachite green in 6 N sulfuric acid, and solution C was 11% (v/v) Tween-20. A 5× working solution was prepared immediately prior to the experiment by mixing 2.5 mL solution A, 10 mL solution B, and 0.2 mL solution C. 6 μL of this working solution was mixed with 24 μL of quenched reaction sample or phosphate standard in a 384-well microplate, incubated at room temperature for 15 min, and

absorbance at 620 nm was measured. ATP hydrolysis rates were calculated by constructing a standard curve and calculating organic phosphate concentrations across reaction time points. nCoMET assays were performed as described[3] in PD buffer containing 20 mM $CoCl_2$ in place of $MgCl_2$.

For substrate-binding experiments, increasing concentrations of quencher-labeled titin^{I27}-ssrA were incubated with a fixed concentration of an Alexa 555-labeled ClpX variant (25 nM) for ~5 min in the presence of ATP (10 mM), ATPγS (1 mM), or no nucleotide and the fluorescence emission spectra (excitation 485 nm; emission 520-530 nm) was averaged across the emission range.

To assay the binding of different concentrations of ClpX variants to Y60W ClpP (25 nM tetradecamer, 50 nM binding sites), samples were incubated for ~5 min in PD buffer plus 2 mM ATP, the tryptophan-emission spectrum (excitation 295 nm; emission 345-360 nm) was averaged for across the emission range, and the center of spectral mass was calculated, plotted against ClpX concentration, and fitted to a quadratic equation for near-stoichiometric binding. Signal to noise did not allow concentrations of Y60W ClpP below 25 nM.

Degradation of unfolded titin^{I27}-ssrA was measured by increases in fluorescence anisotropy[3]. Reactions contained 2 μM titin^{I27}-ssrA unfolded by reaction with fluorescein-iodoacetamide and 18 μM titin^{I27}-ssrA unfolded by carboxymethylation, 0.3 μM ClpX pseudohexamer and 0.9 μM $ClpP_{14}$. Arc(R23C)-Gcn4-ssrA dimers were labeled with either Alexa 488 or Alexa 647 and then allowed to equilibrate to form an equilibrium mixture of homodimers and heterodimers. ClpX (0.1 μM pseudohexamer) variants and $ClpP_{14}$ (0.3 μM) were added together with ATP and a regeneration system (16 mM phosphocreatine, 0.032 mg/mL creatine kinase; Sigma) and the decrease in fluorescence (excitation 494 nm; emission 668 nm) caused by loss of FRET was measured to determine the degradation rate.

Analytical size-exclusion chromatography of 100 μL samples (1.5 μM pseudo hexamer) was performed on a Superdex 200 10/300 GL column (GE Healthcare) in 10 mM HEPES (pH 7.0), 100 mM KCl, 5 mM $MgCl_2$, and 500 μM ATP. Circular-dichroism spectroscopy was performed on an Aviv Model 420 CD spectrometer at 22 °C, using a 1.0 mm path-length quartz cuvette containing protein (400 nM pseudo hexamer) in 10 mM potassium phosphate (pH 7.0). Thermofluor protein-denaturation assays were performed as described[28]. Briefly, 25 μL samples containing 0.2 μM pseudo hexamer in PD buffer, 5× SYPRO Orange, and 5 mM ATP when present were placed in a 96-well PCR plate. SYPRO Orange fluorescence was recorded in a Light Cycler 480 Real Time PCR instrument as samples were heated from 25 to 90 °C at a rate of 1 °C/min.

Supplementary Material

Refer to Web version on PubMed Central for supplementary material.

ACKNOWLEDGMENTS

This research was supported by the US National institutes of Health grant GM-101988 (R.T.S.). B.M.S. was supported by a Massachusetts Institute of Technology Poitras predoctoral fellowship. T.A.B. is supported as an employee of the Howard Hughes Medical Institute.

REFERENCES

1. Baker TA, Sauer RT. ClpXP, an ATP-powered unfolding and protein-degradation machine. Biochim. Biophys. Acta. 2011; 1823:15–28. [PubMed: 21736903]
2. Hersch GL, Burton RE, Bolon DN, Baker TA, Sauer RT. Asymmetric interactions of ATP with the AAA+ ClpX6 unfoldase: allosteric control of a protein machine. Cell. 2005; 121:1017–1027. [PubMed: 15989952]
3. Stinson BM, et al. Nucleotide Binding and Conformational Switching in the Hexameric Ring of a AAA+ Machine. Cell. 2013; 153:628–639. [PubMed: 23622246]
4. Glynn SE, Martin A, Nager AR, Baker TA, Sauer RT. Structures of asymmetric ClpX hexamers reveal nucleotide-dependent motions in a AAA+ protein-unfolding machine. Cell. 2009; 139:744–756. [PubMed: 19914167]
5. Smith DM, Fraga H, Reis C, Kafri G, Goldberg AL. ATP binds to proteasomal ATPases in pairs with distinct functional effects, implying an ordered reaction cycle. Cell. 2011; 144:526–538. [PubMed: 21335235]
6. Sauer RT, Baker TA. AAA+ proteases: ATP-fueled machines of protein destruction. Annu. Rev. Biochem. 2011; 80:587–612. [PubMed: 21469952]
7. Martin A, Baker TA, Sauer RT. Rebuilt AAA+ motors reveal operating principles for ATP-fuelled machines. Nature. 2005; 437:1115–1120. [PubMed: 16237435]
8. Wojtyra UA, Thibault G, Tuite A, Houry WA. The N-terminal zinc binding domain of ClpX is a dimerization domain that modulates the chaperone function. J. Biol. Chem. 2003; 278:48981–48990. [PubMed: 12937164]
9. Popp MW, Antos JM, Grotenbreg GM, Spooner E, Ploegh HL. Sortagging: a versatile method for protein labeling. Nat. Chem. Biol. 2007; 3:707–708. [PubMed: 17891153]
10. Kim YI, et al. Molecular determinants of complex formation between Clp/Hsp100 ATPases and the ClpP peptidase. Nat. Struct. Biol. 2001; 8:230–233. [PubMed: 11224567]
11. Joshi SA, Hersch GL, Baker TA, Sauer RT. Communication between ClpX and ClpP during substrate processing and degradation. Nat. Struct. Mol. Biol. 2004; 11:404–411. [PubMed: 15064753]
12. Kenniston JA, Baker TA, Fernandez JM, Sauer RT. Linkage between ATP consumption and mechanical unfolding during the protein processing reactions of an AAA+ degradation machine. Cell. 2003; 114:511–520. [PubMed: 12941278]
13. Taraska JW, Puljung MC, Olivier NB, Flynn GE, Zagotta WN. Mapping the structure and conformational movements of proteins with transition metal ion FRET. Nat. Methods. 2009; 6:532–537. [PubMed: 19525958]
14. Burton RE, Baker TA, Sauer RT. Energy-dependent degradation: Linkage between ClpX-catalyzed nucleotide hydrolysis and protein-substrate processing. Protein Sci. 2003; 12:893–902. [PubMed: 12717012]
15. Cordova JC, et al. Stochastic but highly coordinated protein unfolding and translocation by the ClpXP proteolytic machine. Cell. 2014; 158:647–658. [PubMed: 25083874]
16. Aubin-Tam M-E, Olivares AO, Sauer RT, Baker TA, Lang MJ. Single-molecule protein unfolding and translocation by an ATP-fueled proteolytic machine. Cell. 2011; 145:257–267. [PubMed: 21496645]
17. Sen M, et al. The ClpXP protease unfolds substrates using a constant rate of pulling but different gears. Cell. 2013; 155:636–646. [PubMed: 24243020]
18. Maillard RA, et al. ClpX(P) generates mechanical force to unfold and translocate its protein substrates. Cell. 2011; 145:459–469. [PubMed: 21529717]
19. Kenniston JA, Baker TA, Sauer RT. Partitioning between unfolding and release of native domains during ClpXP degradation determines substrate selectivity and partial processing. Proc. Natl. Acad. Sci. USA. 2005; 102:1390–1395. [PubMed: 15671177]
20. Thibault G, Houry WA. Role of the N-terminal domain of the chaperone ClpX in the recognition and degradation of lambda phage protein O. J. Phys. Chem. B. 2012; 116:6717–6724. [PubMed: 22360725]

21. Lander GC, et al. Complete subunit architecture of the proteasome regulatory particle. Nature. 2012; 482:186–191. [PubMed: 22237024]
22. Matyskiela ME, Lander GC, Martin A. Conformational switching of the 26S proteasome enables substrate degradation. Nat. Struct. Mol. Biol. 2013; 20:781–788. [PubMed: 23770819]
23. Beckwith R, Estrin E, Worden EJ, Martin A. Reconstitution of the 26S proteasome reveals functional asymmetries in its AAA+ unfoldase. Nat. Struct. Mol. Biol. 2013; 20:1164–1172. [PubMed: 24013205]
24. Chen I, Dorr BM, Liu DR. A general strategy for the evolution of bond-forming enzymes using yeast display. Proc. Natl. Acad. Sci. USA. 2011; 108:11399–11404. [PubMed: 21697512]
25. Kim YI, Burton RE, Burton BM, Sauer RT, Baker TA. Dynamics of substrate denaturation and translocation by the ClpXP degradation machine. Mol. Cell. 2000; 5:639–648. [PubMed: 10882100]
26. Nørby JG. Coupled assay of Na+,K+-ATPase activity. Meth. Enzymol. 1988; 156:116–119. [PubMed: 2835597]
27. Geladopoulos TP, Sotiroudis TG, Evangelopoulos AE. A malachite green colorimetric assay for protein phosphatase activity. Anal. Biochem. 1991; 192:112–116. [PubMed: 1646572]
28. Lavinder JL, Hari SB, Sullivan BJ, Magliery TJ. High-throughput thermal scanning: a general, rapid dye-binding thermal shift screen for protein engineering. J. Am. Che. Soc. 2009; 131:3794–3795.

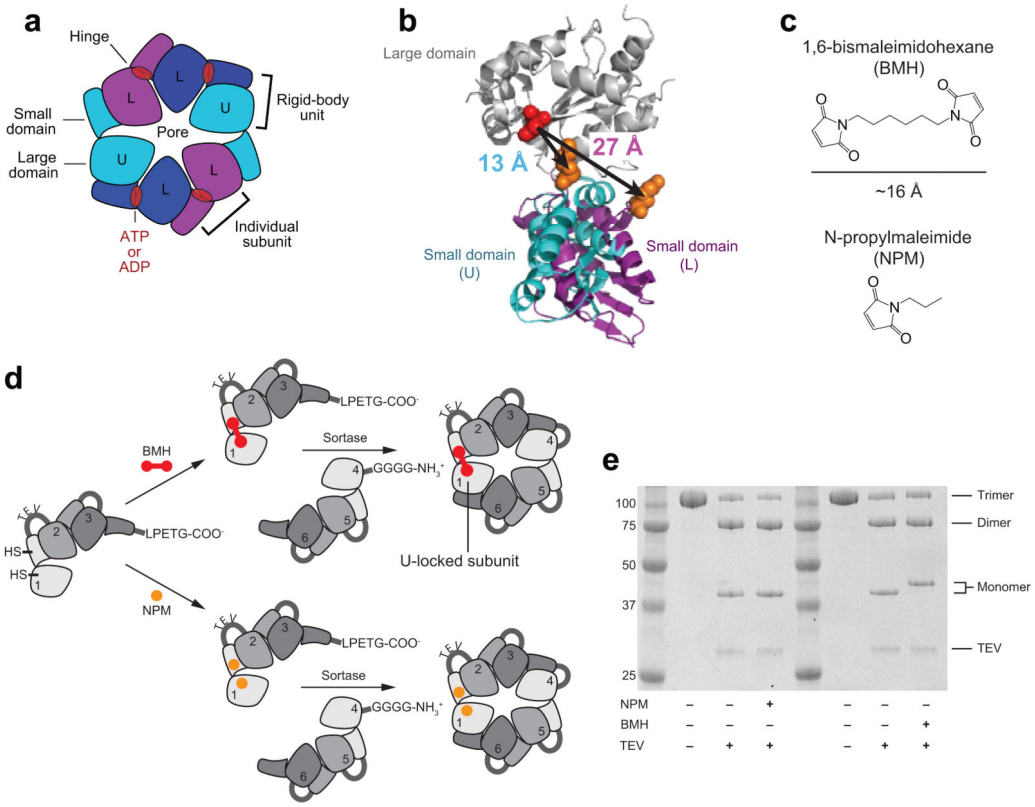

Figure 1.

ATP binding and subunit conformations in ring hexamers of ClpX. (**a**) In most crystal structures, differences in the orientation of the large and small AAA+ domains result in four L subunits that bind nucleotide and two U subunits that do not bind nucleotide. Because each small AAA+ domain packs in a rigid-body interaction with the large AAA+ domain of its clockwise neighbor, nucleotide-dependent changes in the conformation of any subunit are propagated around the topologically closed ring. (**b**) Structures of an L and U subunit (PDB code, 4I81) aligned by their large domains (gray). The beta carbons of D144 and K330 are separated by ~13 Å in U subunits (cyan) and ~27 Å in L subunits (purple). (**c**) Bifunctional (BMH; top) or monofunctional (NPM; bottom) maleimides used to crosslink or modify D144C and K330C in ClpX variants. (**d**) Construction of modified covalent hexamers. See Online Methods for details. (**e**) SDS-PAGE after TEV digestion of ClpX covalent trimers containing one NPM/BMH modified subunit. The uncropped gel is shown in Supplementary Data Set 1.

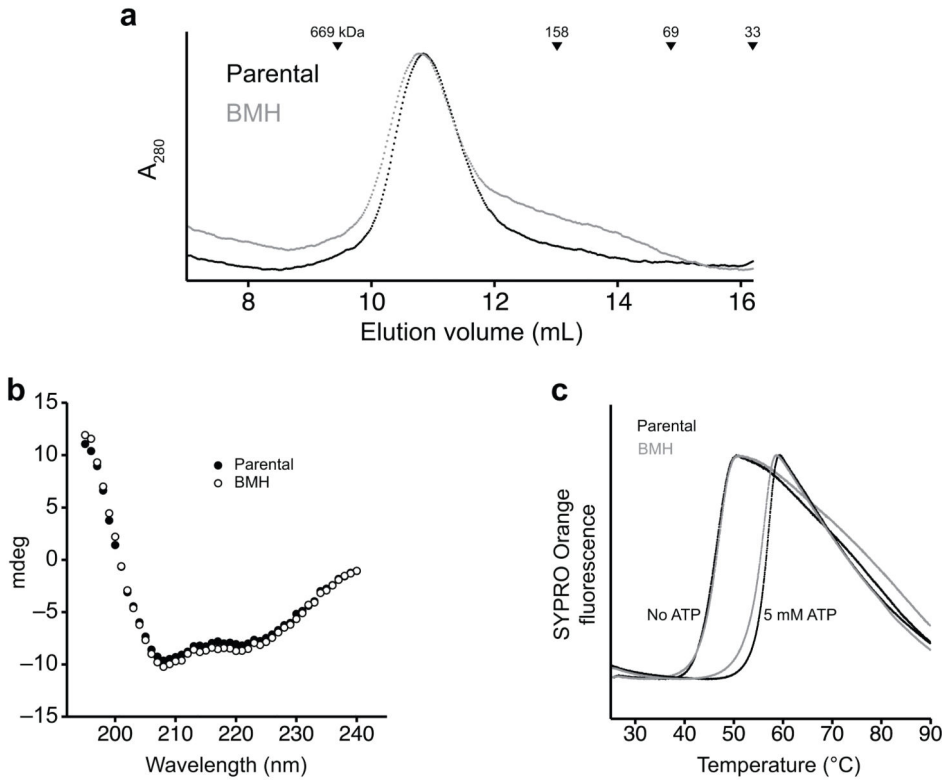

Figure 2.

Physical characterization of parental and BMH enzymes. (**a**) Analytical size-exclusion chromatography of parental and BMH enzymes (100 μL of 1.5 μM pseudo hexamer) in buffer supplemented with 500 μM ATP. (**b**) Circular-dichroism spectra of parental and BMH enzymes (400 nM pseudo hexamer) in ATP-free buffer. (**c**) Thermal denaturation of parental and BMH enzymes (200 nM pseudo hexamer) in buffers with and without 5 mM ATP.

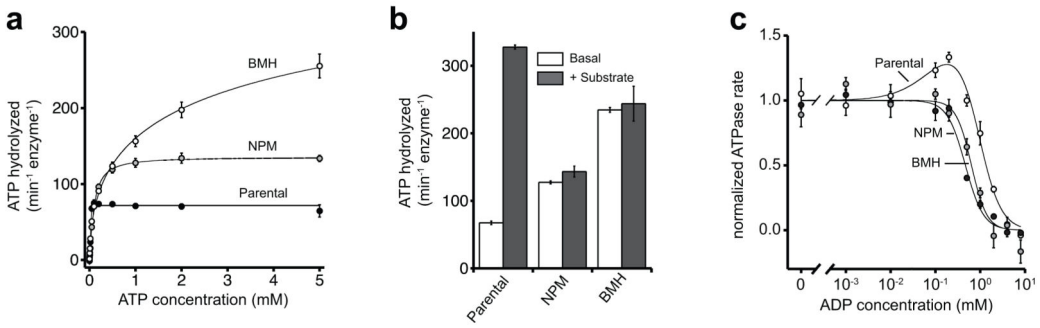

Figure 3.

ATP hydrolysis. (**a**) ATP hydrolysis by parental and BMH or NPM modified ClpX variants (50 nM). (**b**) Rates of hydrolysis of 5 mM ATP by parental and NPM or BMH ClpX variants (50 nM) in the absence and presence of unfolded titin^{I27}-ssrA protein substrate (20 μM). (**c**) Inhibition of hydrolysis of ATP (2 mM) by different concentrations of ADP for parental and NPM or BMH variants (50 nM). Rates are normalized to the rate in the absence of ADP. For the NPM or BMH variants, the lines are fits to the equation $(1 - [ADP]^n/([ADP]^n + IC_{50}{}^n))$. For the parental enzyme, the line is a fit to a biphasic binding equation $(1+a*[ADP]/([ADP]+K_1)-(1+a)*[ADP]^n/([ADP]^n+K_2{}^n))$. IC_{50} values are shown in Table 1. For all panels, values represent means with s.d. error bars (N = 3 technical replicates).

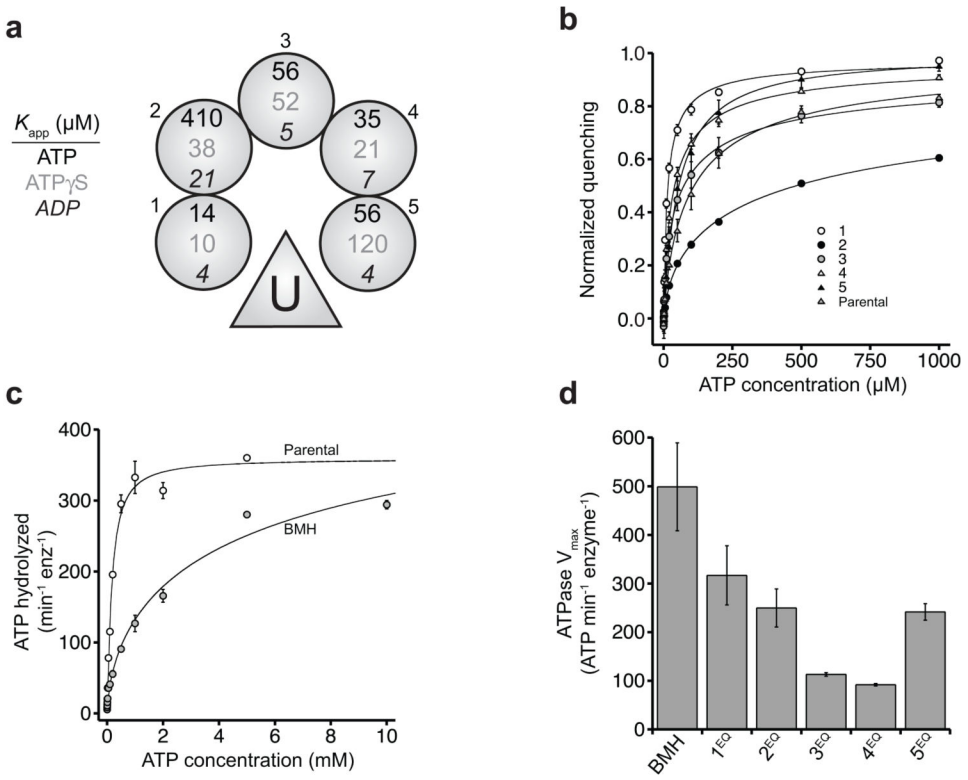

Figure 4.

Subunit-specific nucleotide binding and effects on ATP hydrolysis in BMH U-locked hexamers. (**a**) Apparent ATP, ATPγS and ADP affinities determined by nCOMET experiments for one subunit of the parental enzyme and each unlocked subunit of BMH ClpX (100 nM). Labeled unlocked subunits are numbered based on their clockwise position from the U-locked subunit. K_{app} was determined using fits to the Hill equation (y = amplitude•[nuc]^n/([nuc]^n + K_{app}^n)). Errors in K_{app} were estimated as ±50% based on measurements from duplicate protein preparations. Values of *n* are shown in Table 1. (**b**) ATP binding isotherms for parental and BMH variants, numbered as in panel **a**. Values represent means with s.d. error bars (N = 3 technical replicates). (**c**) ATP hydrolysis supported by 20 mM Co^{2+} for parental and BMH enzymes (25 nM pseudohexamer). Solid lines are fits to [ATP]^n/([ATP]^n + K_M^n). Fitted parameters are shown in Table 1. Values represent means with error bars spanning the range of measured values (N = 2 technical replicates). (**d**) V_{max} values for ATP hydrolysis by single BMH and variants (50 nM) with a single E185Q mutation in one of the five unlocked subunits derived from fits of Michaelis-Menten plots to V_{max} = ([ATP]^n/([ATP]^n + K_M^n)/[enz]. Fitted parameters are shown in Table 1. Error bars, standard error of the nonlinear least-squares regression (N = 3 technical replicates).

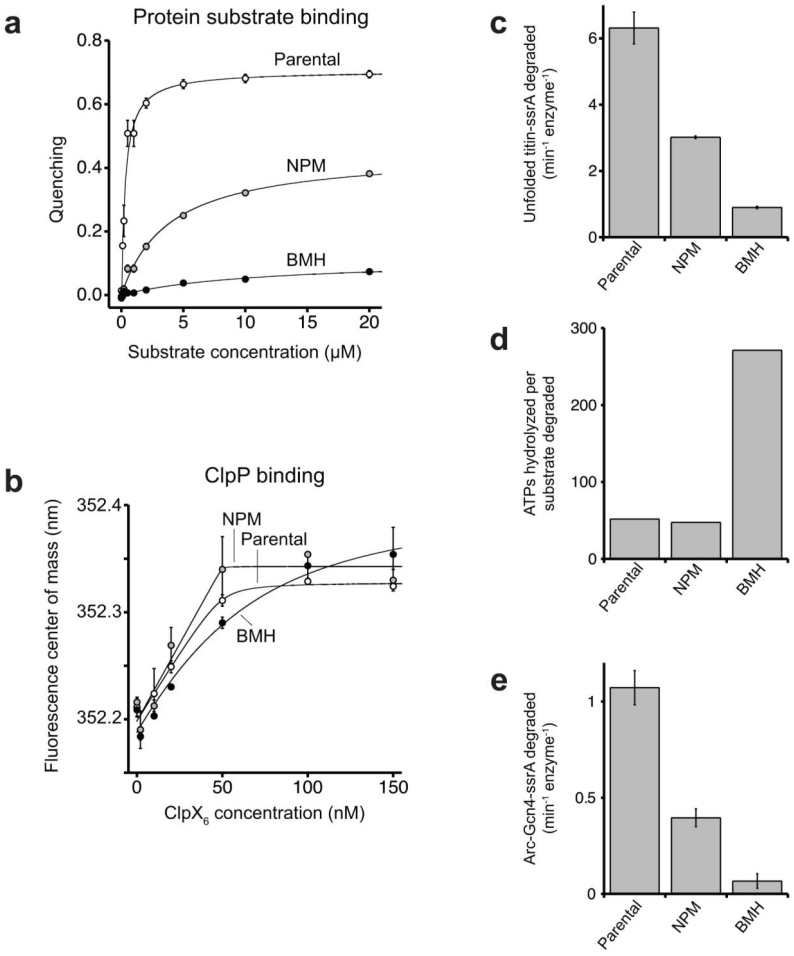

Figure 5.

Binding, unfolding, and degradation of protein substrate by ClpX variants. (**a**) Binding of quencher-labeled titin^{I27}-ssrA to ClpX variants labeled with Alexa 555 at D170C (25 nM; 10 mM ATP). Solid lines are fits to a hyperbolic equation. Apparent affinities and amplitudes are shown in Table 1. Values represent means with error bars spanning the range of measured values (N = 2 technical replicates). (**b**) Binding of parental and NPM or BMH variants to Y60W $ClpP_{14}$ (25 nM) in the presence of 2 mM ATP. Solid lines are fits to a quadratic equation for near stoichiometric binding. K_D's were less than 25 nM for all variants. Values represent means with error bars spanning the range of measured values (N = 2 technical replicates). (**c**) Rates of degradation of unfolded titin^{I27}-ssrA (20 μM) by parental and NPM or BMH enzymes (300 nM) and $ClpP_{14}$ (900 nM). Values are shown in Table 1. Values represent means with error bars spanning the range of measured values (N = 2 technical replicates). (**d**) Energetic efficiency of unfolded titin^{I27}-ssrA degradation calculated as the ratio of the ATPase rate in the presence of unfolded titin^{I27}-ssrA (Fig. 2b) to the rate of degradation in panel A. (**e**) Degradation of dimeric Arc-Gcn4-ssrA (15 μM dimer) by parental and NPM/BMH enzymes (100 nM) and $ClpP_{14}$ (300 nM). Values are shown in Table 1. Values represent means with s.d. error bars (N = 3 technical replicates).

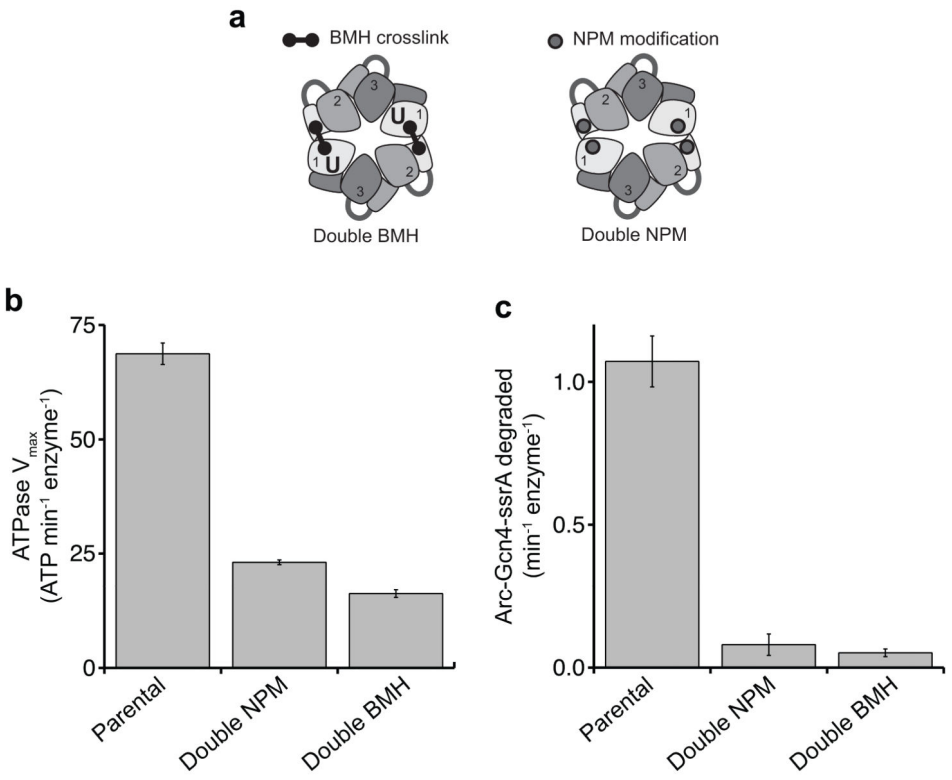

Figure 6.

ATP hydrolysis and degradation by ClpX variants containing two NPM- or BMH-modified subunits. (**a**) Cartoon representations of variants. The pseudo hexamer containing two NPM-modified subunits is termed “double NPM” and that the one containing two BMH-modified subunits is termed “double BMH”. (**b**) V_{max} values for ATP hydrolysis by parental and double NPM/BMH enzymes (50 nM) derived from fits of Michaelis-Menten plots to $V_{max} = ([ATP]^n/([ATP]^n + K_M^n)/[enz]$. Error bars, standard error of the nonlinear least-squares regression (N = 3 technical replicates). (**c**) Degradation of dimeric Arc-Gcn4-ssrA (15 μM dimer) by parental and double NPM/BMH enzymes (100 nM) and $ClpP_{14}$ (300 nM). ATP concentration was 10 mM. Values represent means with s.d. error bars (N = 3 technical replicates).

Table 1
Nucleotide binding, hydrolysis, and protein-substrate activities

Parameters were determined by nonlinear least-squares fitting of experimental data as described in figure legends. Errors are standard errors of the regression. For ADP-inhibition experiments, IC_{50} is defined as the concentration of ADP resulting in 50% hydrolysis relative to the initial rate. For nCoMET experiments, errors in K_{app} are estimated as ±50% on the basis of independent protein preparations.

ATP hydrolysis

	V_{max} (ATP min^{-1} $enzyme^{-1}$)	K_M (μM)	*n*
parental	69 ± 2	25 ± 2	3.6 ± 0.9[a]
NPM	136 ± 2	94 ± 2	1.2 ± 0.1
BMH	500 ± 90	4000 ± 3000	0.5 ± 0.1
1EQ	320 ± 60	2000 ± 1000	0.5 ± 0.1
2EQ	250 ± 40	4000 ± 2000	0.5 ± 0.1
3EQ	113 ± 4	140 ± 10	0.9 ± 0.1
4EQ	92 ± 2	180 ± 10	1.0 ± 0.1
5EQ	240 ± 20	1000 ± 200	0.6 ± 0.1
parental (Co^{2+})[b]	340 ± 10	170 ± 20	1.3 ± 0.2
BMH (Co^{2+})[b]	420 ± 90	3000 ± 2000	0.8 ± 0.1

ADP inhibition

	IC_{50} (mM)
parental	1.4
NPM	0.5
BMH	0.6

nCoMET

	ATP		ATPγS		ADP	
	K_{app} (μM)	*n*	K_{app} (μM)	*n*	K_{app} (μM)	*n*
parental	102	0.8 ± 0.1	11	1.0 ± 0.1	13	0.6 ± 0.1
subunit 1	14	0.8 ± 0.1	10	1.1 ± 0.1	4	0.9 ± 0.1
subunit 2	410	0.6 ± 0.1	38	0.8 ± 0.1	21	0.6 ± 0.1
subunit 3	56	0.6 ± 0.1	52	0.6 ± 0.1	5	0.6 ± 0.1
subunit 4	35	0.8 ± 0.1	21	0.8 ± 0.1	7	0.7 ± 0.1
subunit 5	56	1.0 ± 0.1	120	0.7 ± 0.1	4	0.9 ± 0.1

protein substrate binding

	K_{app} (μM)	maximal quenching
parental	0.32 ± 0.05	0.71 ± 0.02
NPM	3.8 ± 0.5	0.45 ± 0.02
BMH	11 ± 4	0.11 ± 0.02

protein substrate degradation

	unfolded titin-ssrA (min^{-1} $enzyme^{-1}$)	Arc-Gcn4-ssrA (min^{-1} $enzyme^{-1}$)
parental	6.3 ± 0.7	1.1 ± 0.1
NPM	3.0 ± 0.1	0.40 ± 0.05
BMH	0.90 ± 0.05	0.07 ± 0.04

[a] Lower values of the Hill constant (~1.4) were observed in experiments containing saturating protein substrate[3], which was not present in these experiments.

[b] Parameters for experiments shown in Fig. 4c, which were performed in the presence of Co^{2+} rather than Mg^{2+} for comparison to nCoMET experiments.

Table 2

Nucleotide K_{app} values averaged over all subunits

	Parental average K_{app} (μM)	BMH average K_{app} (μM)
ATP	102	113
ATP©S	11	8
ADP	13	8